

The Ionization of Accretion Flows in High Mass Star Formation: W51e2

Eric Keto¹ and Pamela Klaassen²

*Harvard-Smithsonian Center for Astrophysics, 60 Garden Street, Cambridge, MA 02138,
USA*

Dept. of Physics & Astronomy, McMaster University, Hamilton, ON

ABSTRACT

Previous observations show that the hypercompact HII region W51e2 is surrounded by a massive molecular accretion flow centered on the HII region. New observations of the H53 α radio recombination line made with the VLA at 0.45 arc second angular resolution show a velocity gradient in the ionized gas within the HII region of $> 500 \text{ kms}^{-1} \text{ pc}^{-1}$ comparable to the velocity gradient seen in the molecular accretion flow. New CO line observations made with the SMA at arc second angular resolution detect a molecular bipolar outflow immediately around the W51e2 HII region and extending along the axis of rotation of the molecular flow. These observations are consistent with an evolutionary phase for high mass star formation in which a newly formed massive star first begins to ionize its surroundings including its own accretion flow.

Subject headings: HII Regions

1. Introduction

1.1. HII regions within star-forming accretion flows

Molecular line observations of several massive-star forming regions show evidence for star-forming accretion flows around small HII regions (Guilloteau et al. 1983; Ho & Haschick 1986; Keto et al. 1987a,b, 1988; Ho & Young 1996; Zhang & Ho 1997; Young et al. 1998; Zhang et al. 1998; Sollins et al. 2004, 2005a,b; Beltran et al. 2006). These HII regions (W3(OH),

¹keto@cfa.harvard.edu

²klaassp@physics.mcmaster.ca

G10.6-0.4, W51e2, G28.20-0.04, and G24.78+0.08) are of hypercompact (HC) or ultracompact (UC) size and are bright enough to require an ionizing flux at a level produced only by one or more O-type stars. Thus the presence and brightness of the HII regions at the centers of these flows indicate that the accretion is associated with the formation of the most massive stars.

The presence of the HII regions within molecular accretion flows poses some simple yet interesting questions. How does the development of an HII region affect accretion and the evolution of a young star? Does the formation of an HII region prevent further accretion and growth of the star? How does an HII region affect a pre-existing, bipolar outflow (BPO) of the type that is typically associated with the star-forming accretion flows of lower mass stars?

The interaction of HII regions with accretion flows and associated BPOs occurs in an evolutionary phase in massive star formation common to all young O stars. Stellar structure calculations indicate that massive stars with accretion rates similar to those observed around the HII regions listed above ($10^{-3} - 10^{-2} M_{\odot} \text{ yr}^{-1}$, (Keto 2002a, table 1)) should begin core nuclear burning at a mass well below that of an O star (Stahler, Shu & Taam 1980, 1981a,b; Palla & Stahler 1993; Beech & Mitalas 1994; Norberg & Maeder 2000; Behrend & Maeder 2001; Keto & Wood 2006). These calculations also indicate that the temperature and luminosity of the accreting star is about the same as a ZAMS star of equivalent mass. Thus an accreting star begins to produce an HII region once the star reaches a mass, temperature and luminosity equivalent to early B, about 15 - 20 M_{\odot} . If the star is to accrete the additional mass to become an O star, then the accretion must continue past the mass when an HII region to forms. Thus the interaction of accretion flows and HII regions is inevitable in the early evolution of massive stars; however, this interaction is currently not well understood.

Since bipolar outflows are invariably associated with star-forming accretion flows of lower mass stars up to later-type B, an HII region that develops within a pre-existing molecular accretion flow must also interact with the molecular bipolar outflow that we expect to be associated with the accretion flow. There are few detections of outflows from young O stars. Young O stars are rare both because of the steep stellar mass spectrum and because of the short time that they spend in the accretion phase. Furthermore, they are difficult to identify because they are deeply embedded in molecular clouds and always at kpc distances. Maybe we have not yet found enough examples, or maybe the HII regions that surround all young O stars modify or terminate the outflows.

1.2. The ionized accretion flows

Of the HII regions associated with molecular accretion flows, three have been observed in radio recombination lines (RRL) with high enough angular resolution to map the velocities of the ionized gas within the HII regions. All three HII regions show rotation in the ionized gas and one also shows infall. The similarities of the velocities in the molecular and ionized phases suggest that the flow is continuous across the ionization boundary. The UCHII region G10.6-0.04 which contains a small group of O stars is the best studied example, and the one that also shows an inward flow of the ionized gas (Keto 2002a; Keto & Wood 2006). The G34.3+0.2 HII region shows rotation in its cometary shaped ionized outflow (Garay et al. 1986) that is perpendicular to a rotationally flattened molecular accretion flow (Keto et al. 1987b). More recently, Sewilo et al. (2007) report evidence for rotation of the ionized gas within the G28.20-0.04 HII region in the same orientation and velocities as the rotation seen in the “97 kms⁻¹” component of the NH₃(3,3) line previously mapped by Sollins et al. (2005b). In addition to these three, rotation of the ionized gas within the G45.07+0.13 HII region is also reported in Garay et al. (1986), but observations of the surrounding molecular gas are inconclusive as to the presence of a molecular accretion flow (Cesaroni et al. 1994; Wilner et al. 1996).

Inward flowing ionized gas has been observed only in the large, cluster-scale HII region G10.6-0.4. This HII region is the only one of the three observed examples that has sufficient stellar mass inside the HII region (a few hundred M_⊙) that the Bondi-Parker transonic radius $R_g = GM/2c_s^2$ is large enough (several thousand AU) to be observationally resolved at the distances (6 - 8 kpc) of these three HII regions. The other two HII regions might also have inward flowing ionized gas, but if they contain only one O star or even a binary or triple, then the inward flow will be on a length scale that is too small to resolve observationally.

1.3. The massive bipolar outflows

There have been a few single dish telescope surveys that study BPOs in star forming regions with UC and HC HII regions. Shepherd & Churchwell (1996) and Klaassen & Wilson (2007) looked for BPOs in massive star-forming regions with UC/HC HII regions. Shirley et al. (2003) selected star-forming regions with water maser emission. Because water masers are associated with high mass stars, these regions also often contain UC or HC HII regions. These surveys detect BPOs with mass outflow rates and energies that indicate that they are driven by massive stars. However, these single dish observations do not have the angular resolution necessary to determine whether the BPOs are associated with the bright HII regions and therefore O stars or with other nearby massive stars currently equivalent to ZAMS B

without HII regions. In order to determine whether a BPO is associated with a particular accreting massive star or an HII region, we need higher resolution spectral line observations around the HII region in molecules that best trace bipolar outflows.

2. New observations

We chose to observe the W51e2 HII region because of its well-studied molecular accretion flow (Rudolph et al. 1990; Ho & Young 1996; Zhang & Ho 1997; Zhang et al. 1998; Sollins et al. 2004; Young et al. 1998). In this paper we report on VLA observations of the H53 α radio recombination line (RRL) and on SMA observations of CO(J=2-1). We observed the highest frequency RRL accessible by the VLA because the higher frequency lines have lower optical depth, and we can observe the velocities of the gas deeper inside the HII region. We observed the CO in a transition above the ground state and at $\sim 1''$ angular resolution to improve the likelihood of observing a BPO associated with hot molecular gas near the HII region.

2.1. Experimental setup

Our H53 α observations of the ionized gas in W51e2 were made at the National Radio Astronomy Observatory Very Large Array (VLA)¹. The H53 α line was observed in the C array at a resolution of 0.45''. The ¹²CO(J=2-1) line was observed at the Submillimeter Array (SMA)² in its extended configuration, resulting in a spatial resolution of $\sim 1''$. The CO line was detected simultaneously with H30 α , and both sets of observations are described in Keto, Zhang & Kurtz (2008). The James Clerk Maxwell Telescope³ was used to observe the larger scale structure of the molecular gas, and these observations were combined with the SMA observations using the non-linear image combination program MOSMEM in the MIRIAD data reduction package (as described in Klaassen et al. in prep).

¹The National Radio Astronomy Observatory is a facility of the National Science Foundation operated under cooperative agreement by Associated Universities, Inc.

²The Submillimeter Array is a joint project between the Smithsonian Astrophysical Observatory and the Academia Sinica Institute of Astronomy and Astrophysics, and is funded by the Smithsonian Institution and the Academia Sinica.

³The James Clerk Maxwell Telescope is operated by The Joint Astronomy Centre on behalf of the Science and Technology Facilities Council of the United Kingdom, the Netherlands Organisation for Scientific Research, and the National Research Council of Canada.

2.2. The ionized flow

Figure 1 shows the average velocity of the H53 α line. The velocity gradient is approximately 8 kms⁻¹ between 57 and 65 kms⁻¹ VLSR with a position angle -30° (west of North). This velocity pattern is consistent with either rotation or outflow. We prefer the interpretation that the H53 α velocities indicate rotation for a couple of reasons. First, the observed velocity gradient is perpendicular to the CO outflow. Bipolar outflows associated with lower mass stars are always oriented approximately perpendicular to the rotation. Second, the interpretation of rotation is consistent with the magnitude and direction of the rotational velocity gradient observed in NH₃ and CH₃CN (Zhang & Ho 1997; Zhang et al. 1998).

The clearest signature of rotation in the molecular gas is in figure 7 of Zhang & Ho (1997) in the position-velocity diagram of NH₃(3,3) along a line at position angle of 135° , and consistent ($135 - 180 = -55^\circ$) with the position-angle of the velocity gradient in the ionized gas (-30°). We prefer to use the NH₃(3,3) line in this interpretation rather than the (2,2) line because the higher excitation line should derive from gas closer to the hot HII region. However, there is considerable uncertainty in locating the exact angle of the axis of rotation using the molecular line observations. These observations map the flow at relatively large scales before the accretion has spun-up by angular momentum conservation to higher rotational velocities. The observed infall velocities are comparable or greater than the rotational velocities, and the rotational component is difficult to extract. For example, comparison of the position angle (-55°) of the rotational gradient derived from the NH₃ observations with the position angle (-70°) derived from CH₃CN (Zhang et al. 1998) suggests an uncertainty of several tens of degrees.

Our observations do not fully resolve the HII region, but the 1.3 cm continuum observation of Keto, Zhang & Kurtz (2008) indicates a FWHM of $0.4''$ similar to the upper limit estimated by Zhang & Ho (1997) and Scott (1978). The radius, R , associated with the velocity difference ΔV , is uncertain because of our low angular resolution. So we use the FWHM of the continuum emission as a characteristic size. Assuming that the observed velocities are rotational, the mass of the star within the W51e2 region is estimated as $M = \Delta V^2 R / 2G$. Assuming a distance of 8 kpc, we derive a lower limit to the velocity gradient of > 500 kms⁻¹ pc⁻¹ and a dynamical mass of $V^2 R / 2G > 15 M_\odot$. This mass is roughly consistent with a previous estimate of about $20 M_\odot$ derived from the emission measure of the radio continuum (Scott 1978).

This estimated velocity gradient in the ionized gas is similar to that measured in molecular gas. Zhang & Ho (1997) measure a velocity gradient in NH₃ of 500 kms⁻¹ pc⁻¹ centered around 58 kms⁻¹ VLSR. Owing to limited angular resolution, the exact value of the velocity gradient may be somewhat uncertain. Zhang et al. (1998) derive a lower value (100 kms⁻¹

pc^{-1}) for the velocity gradient from observations of CH_3CN . Nonetheless, the similarity in the magnitude and direction of the velocity gradients observed in the molecular and ionized gas suggests that there is a continuous flow of gas from the molecular to the ionized phase such that the ionized gas retains some memory of the velocities of the molecular accretion flow.

2.3. The bipolar outflow

Figure 2 shows the bipolar outflow in CO. The orientation of the flow is along the rotation axis of the ionized and molecular accretion flows defined by the $\text{H}53\alpha$ RRL and NH_3 observations of (Zhang & Ho 1997). The outflow is seen as blue and red lobes in the maps of integrated emission. In figure 2, the blue lobe is shown in the emission integrated from 20 to 44 kms^{-1} (blue) and the red lobe from 68 to 92 kms^{-1} (red). These ranges are both 24 kms^{-1} wide, starting at velocities $\pm 12 \text{ km s}^{-1}$ from the VLSR of the larger scale molecular gas (56 km s^{-1}). The blue shifted lobe is much brighter than the red one and better collimated. The better collimation of the blue flow results in a smaller volume. If the entrained mass is estimated from the volume and brightness, the two flows have approximately the same mass (3 - 4 M_\odot) and kinetic energy ($\sim 3 \times 10^{43} \text{ J}$), as calculated from zeroth and first moment maps of the outflow (Klaassen et al. in prep).

3. Implications

A conceptual model for the ionized flow in W51e2 may be constructed as a composite of a couple of model calculations in the literature. The expected structure (morphology) of an HII region that develops within a large scale molecular accretion flow may be calculated from ionization balance (Keto 2007). In particular, figure 1c of that paper shows a nearly spherical HII region around a rotationally flattened molecular flow that may be relevant for W51e2. These calculations describe the structures of HII regions but do not calculate the velocities or densities of the ionized gas. Rather they assume an ionized flow based on the Parker wind model (Parker 1958). The velocities and densities of the gas that flows into an HII from a rotationally flattened molecular flow have been calculated in models of photo-evaporating disks (PEDs) (Hollenbach et al. 1994; Yorke 1995; Yorke & Welz 1996; Lizano et al. 1996; Johnstone, Hollenbach, & Bally 1998; Lugo, Lizano & Garay 2004). However, these models do not calculate the structure of the molecular accretion flow and HII region for the types of molecular accretion flows that are observed around HII regions. Rather they assume the accretion flow is in the form of an infinitely thin disk. In the absence of a more complete

calculation we may conceptually combine the flow morphology from Keto (2007) with the velocities and densities from the PED models to interpret the observations of W51e2. The spin-up of the flow seen in the molecular line observations suggests that the large scale molecular accretion flow becomes progressively more flattened at smaller radii. If the flow is sufficiently dense at its mid-plane, it is able to resist ionization and extend into the HII region as described in Keto (2007). Across the top and bottom boundaries of the flattened molecular flow there is an ionization front that continuously supplies gas to the HII region as described in the PED models. Since there is no obvious force to immediately stop the rotation of the gas as it crosses the ionization front, the ionized gas is also rotating. Observations of high frequency RRL such as the H53 α are dominated by the densest gas that is near the ionization front. The velocities of the H53 α line thus show the rotation in the ionized gas coming off the rotating molecular accretion flow.

The density of the ionized gas decreases rapidly as it accelerates off the ionization front around the flattened molecular accretion flow. The exact rate of the density decrease depends on the geometry of the flow. The Parker wind model assumes a purely spherical flow while the PED models describe the flow off a flat, rotating disk. In both cases, the density distribution is approximately exponential (hydrostatic) where the flow velocities are subsonic and closer to a power law past the transonic point. Observations in the radio continuum should thus measure a rising spectral energy distribution (SED) consistent with the steep density gradient in the outflowing ionized wind. In the case of W51e2, the observed SED may be reproduced by a model with a density gradient scaling with radius as the -2.5 power (Keto, Zhang & Kurtz 2008).

The PED models show that the ionized gas flows along the rotation axis, and the structures in Keto (2007) show that this flow can be further channeled by the density structure of the molecular accretion flow. This outflowing ionized gas could drive a molecular BPO, but this BPO would be quite different in collimation and velocity structure from those BPOs associated with the accretion flows of lower mass stars. At the moment, the driver of the BPO that we see in CO is not known. It may be the original BPO, but now flowing through the HII region, or it may be a remnant of a now terminated flow (Klaassen et al. 2006) or it might be driven by the ionized outflow.

4. Conclusions

Our new radio recombination line observations of W51e2 detect rotation in the ionized gas consistent with an accretion flow, and our new CO line observations detect a molecular bipolar outflow along the rotation axis.

The observations are consistent with the structure expected at the time that an accreting massive star begins to ionize its surroundings including the accretion flow responsible for the formation of the star.

REFERENCES

- Beech, M., & Mitalis, R., 1994, *ApJ Suppl.*, 95, 517
- Behrend, A. & Maeder, A., 2001, *AA*, 373, 190
- Beltran, M.T., Cesaroni, R., Codella, C., Testi, L., Furuya, R.S., Olmi, L., 2006, *Nature*, 443, 427
- Cesaroni, R., Churchwell, E., Hofner, P., Walmsley, C.M., & Kurtz, S., 1994, *AA*, 288, 903
- Garay, G., Rodriguez, L.F., van Gorkom, J.H., 1986, 309, 553
- Guilloteau, S., Stier, M.T., & Downes, D., 1983, *AA*, 126, 10
- Ho, P.T.P. & Haschick, A.D., 1986, *ApJ*, 304, 501
- Ho, P.T.P. & Young, L.M., 1996, *ApJ*, 472, 754
- Hollenbach, D., Johnstone, D., Lizano, S., Shu, F., 1994, *ApJ*, 428, 654
- Johnstone, D., Hollenbach, D., & Bally, J., 1998, *ApJ*, 499, 758
- Keto, E., Ho, P.T.P., & Haschick, A.D. 1987a, *ApJ*, 318, 712
- Keto, E., Ho, P.T.P., & Reid, M.J., 1987b, *ApJ*, 323, L117
- Keto, E., Ho, P.T.P., & Haschick, A.D. 1988, *ApJ*, 324, 920
- Keto, E. 2002a, *ApJ*, 568, 754
- Keto, E. 2002b, *ApJ*, 580, 980
- Keto, E. 2003, *ApJ*, 599, 1196
- Keto, E., & Wood, K. 2006, *ApJ*, 637, 850
- Keto, E. 2007, *ApJ*, 666, 976
- Keto, E., Zhang, Q., & Kurtz, S., 2008, *ApJ*, 672,423

- Klaassen, P.D., Plume, R., Ouyed, R., von Benda-Beckmann, 2006, ApJ, 648, 1079
- Klaassen, P.D. & Wilson, C.D., 2007, ApJ, 663, 1092
- Lizano, S., Canto, J., Garay, G., Hollenbach, D., 1996, ApJ, 465, 216
- Lugo, J., Lizano, S., Garay, G., 2004, ApJ, 614, 807
- Norberg, P. & Maeder, A., 2000, AA, 359, 1025
- Palla, F., & Stahler, S., 1993, ApJ, 418, 414
- Parker, E., 1958, ApJ, 128, 664
- Rudolph, A., Welch, W.J., Palmer, P., Dubrulle, B., 1990, ApJ, 363, 528
- Scott, P.F., 1978, MNRAS, 183 435
- Sewilo, M., Churchwell, E., Kurtz, S., Goss, W.M., Hofner, P., 2007, ApJ, submitted
- Shepherd, D.S. & Churchwell, E., 1996, ApJ, 472, 225
- Shirley, Y.L., Evans, N.J., II, Young, K.E., Knez, C., Jaffe, D.T., 2003, ApJS, 149, 375
- Sollins, P.K., Zhang, Q., Ho, P.T.P., 2004, ApJ, 606, 943
- Sollins, P.K., Zhang, Q., Keto, E., Ho, P.T.P., 2005a, ApJ, 624, 49
- Sollins, P.K., Zhang, Q., Keto, E., Ho, P.T.P., 2005b, ApJ, 631, 399
- Stahler, S., Shu, F., Taam, R., 1980, ApJ, 241, 637
- Stahler, S., Shu, F., Taam, R., 1981a, ApJ, 242, 226
- Stahler, S., Shu, F., Taam, R., 1981b, ApJ, 248, 727
- Wilner, D.J., Ho, P.T.P., Zhang, Q., 1996, 462, 339
- Yorke, H. & Welz, A., 1996, A&A, 315, 555
- Yorke, H., 1995, Rev. Mex. AA, 1, 35
- Young, L.M., Keto, E., & Ho, P.T.P. 1998, ApJ, 1998, 507
- Zhang, Q., & Ho, P.T.P 1997, ApJ, 488, 241
- Zhang, Q., Ho, P.T.P., & Ohashi, H. 1998, ApJ, 494, 636

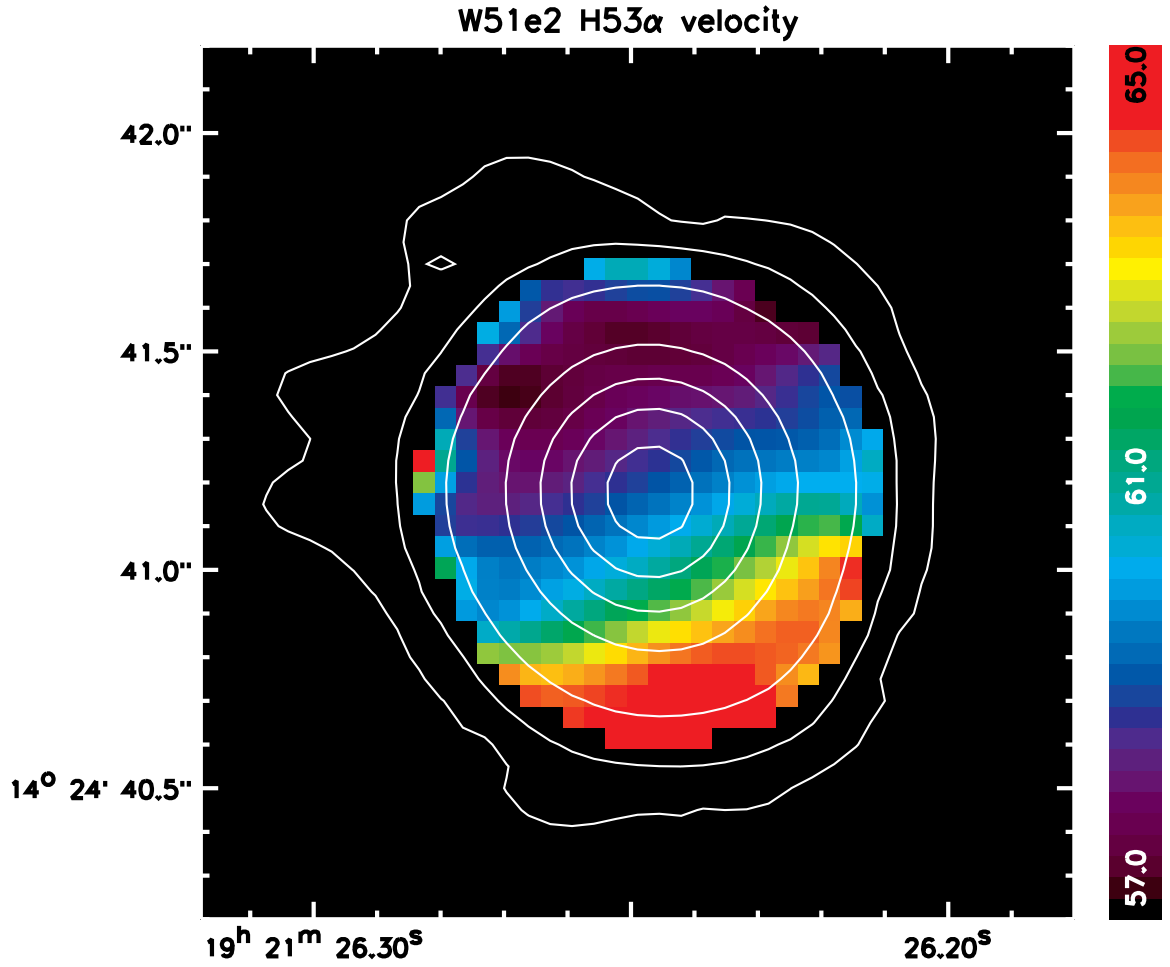


Fig. 1.— Velocity of the H53 α line in W51e2 in color. The color scale ranges from 57 to 65 km s^{-1} . The contours show the 7 mm continuum emission at 2, 4, 10, 30, 50, 70 and 90% of the peak emission of 0.15 Jy/beam. Coordinates are in the B1950 epoch.

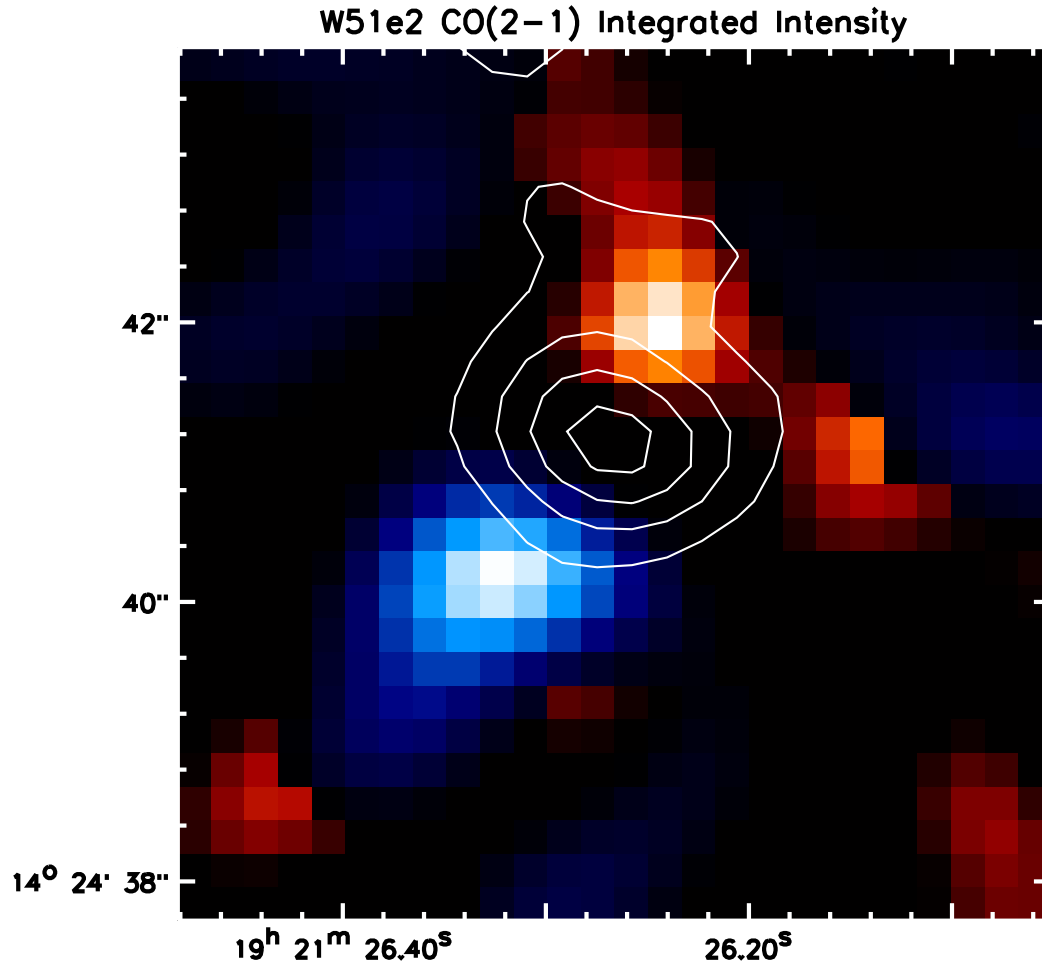


Fig. 2.— Integrated emission of the CO(2-1) line in color. The emission from 20 to 44 kms^{-1} is shown in blue and from 68 to 92 kms^{-1} in red. The blue scale ranges from -17 to 47 K kms^{-1} . The red scale ranges from -9 to 16 K kms^{-1} . The contours show the 1 mm continuum emission at 30, 50, 70 and 90% of the peak emission of 2.1 Jy/beam. This map of W51e2 is on a larger scale than figure 1. Coordinates are in the B1950 epoch.